

Dalton Transactions

Accepted Manuscript



This is an *Accepted Manuscript*, which has been through the Royal Society of Chemistry peer review process and has been accepted for publication.

Accepted Manuscripts are published online shortly after acceptance, before technical editing, formatting and proof reading. Using this free service, authors can make their results available to the community, in citable form, before we publish the edited article. We will replace this *Accepted Manuscript* with the edited and formatted *Advance Article* as soon as it is available.

You can find more information about *Accepted Manuscripts* in the [Information for Authors](#).

Please note that technical editing may introduce minor changes to the text and/or graphics, which may alter content. The journal's standard [Terms & Conditions](#) and the [Ethical guidelines](#) still apply. In no event shall the Royal Society of Chemistry be held responsible for any errors or omissions in this *Accepted Manuscript* or any consequences arising from the use of any information it contains.

Cite this: DOI: 10.1039/c0xx00000x

www.rsc.org/xxxxxx

ARTICLE TYPE

'Aggregation Induced Phosphorescence' Active 'Rollover' Iridium(III) Complex as Multi-Stimuli-Responsive Luminescence Material

Parvej Alam^a, Gurpreet Kaur^b, Shamik Chakraborty^a, Angshuman Roy Choudhury^b, Inamur Rahaman Laskar^{a*}

5

^aDepartment of Chemistry, Birla Institute of Technology and Science, Pilani Campus, Pilani, Rajasthan, India, ir_laskar@bits-pilani.ac.in; ^bDepartment of Chemical Sciences, Indian Institute of Science Education and Research (IISER), Mohali, Sector 81, S. A. S. Nagar, Manauli PO, Mohali, Punjab, 140306, India, angshurc@iisermohali.ac.in

10 Received (in XXX, XXX) Xth XXXXXXXXXX 20XX, Accepted Xth XXXXXXXXXX 20XX

DOI: 10.1039/b000000x

On reaction of 2,2'-bipyridine with iridium(III), an 'aggregation induced phosphorescence (AIP)' active "rollover" complex [Ir(PPh₃)₂(bipy-H)(Cl)(H)], (bpy-H = κ²N,C-2,2'-bipyridine) or [Ir(bipy-H)] was obtained. The emission color changes from bluish-green to yellowish-orange and *vice-versa* after repeated protonation and deprotonation of [Ir(bipy-H)], respectively which invariably supports of its reversible nature. [Ir(bipy-H)] is sensitive to the strength of acids having different pK_a values. The tuning of emission property has been demonstrated with respect to pK_a of different acids. This behavior allow the complex, [Ir(bipy-H)] to function as a phosphorescence acid sensor in both its solution and the solid state as well as a chemosensor for detecting acidic and basic organic vapors. The protonated form, [Ir(bipy-H)H⁺] which is generated after protonation of [Ir(bipy-H)] has been observed to use as a solvatochromic probe for the oxygen containing solvents, and also showing vapochromic property. The emission, absorption and ¹H NMR spectra of [Ir(bipy-H)] under acidic and basic condition demonstrating its reversible nature. The DFT based calculations suggested that the change in electron affinity of pyridinyl ring is responsible for all the processes.

Introduction

25

The past decade research is dedicated to the iridium(III) complexes and its potential application in the field of organic light-emitting diodes (OLEDs)¹, bio- and chemo-sensors² and vapoluminescent materials^{2j-l} because of their intriguing and superior photophysical properties, long luminescence lifetimes³ (100 ns to ms), large Stokes shifts (hundreds of nm) and high quantum yields⁴ in the visible region.

Unfortunately, the most of the metal complexes are suffered from the inherent tendency of the lumophores *i.e.*, concentration quenching (CQ)⁵. In CQ the emission of dilute solution is more emissive than its concentrate solution *i.e.* the emission quenched

with increasing concentration. The main cause of quenching is intermolecular interactions due to formation of aggregate that is why, the CQ has frequently been called "aggregation caused quenching" (ACQ)⁶. It is a deleterious for their potential applications as luminescent materials; hence, it is highly demandable to develop the non ACQ luminophor that can overcome this notorious problem.

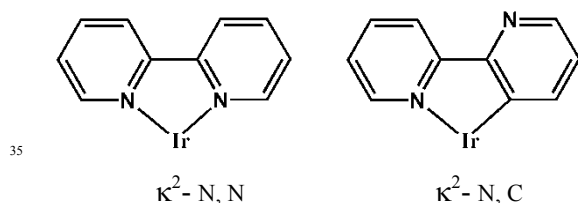
In 2001, Tang *et al* introduced an anti ACQ phenomenon - where the dilute solution was very weak or non luminescent while the emission intensity of concentrate solution was emitting strongly. This "anti ACQ" phenomenon is known as "Aggregation Induced Emission (AIE), *the Whole is more Brilliant than the part*"⁷. Instead of blocking aggregation, a natural and inherent tendency of materials, to actively utilize the aggregation process, shows its

constructive nature. The fantastic discovery of AIE is given tremendous contribution in different high-tech applications, optoelectronic⁸, chemical sensors⁹, biological probes¹⁰, stimuli-responsive nanomaterials¹¹ and the fabrication of non-doped OLEDs¹². The main cause of AIE phenomenon is restriction of intramolecular rotation¹³ (RIR), planarization, J-type aggregates¹⁴, restriction of intramolecular charge transfer¹⁵, E-Z isomerization¹⁶ and twisted intramolecular charge transfer¹⁷ (TICT).

Very recently, Zn(II)¹⁸, Au(I)¹⁹, Pt(II)²⁰, Pd(II)²¹, Os(IV)²², Cu(I)²³ and Ir(III)²⁴ complexes exhibiting the phosphorescent AIE or in better way aggregation induced phosphorescence (AIP) character. But the octahedral Ir(III) complexes having AIP character is still rare²⁵. The synthesis and design of Ir(III) with AIP character has gained increasing attention.

2,2'-Bipyridine (bipy) is one of the most widely used ligands in organometallic chemistry. [Ir(bipy)₃](NO₃)₃ and Ir(bipy)₃(ClO₄)₃ were the first *tris*-2,2'-bipyridyl complexes of iridium reported²⁶ by Flynn and Demas in 1974. The coordination mode of bipyridine in these complexes was observed in bidentate fashion. Along with this monodentate and bridging coordinations are also known.²⁷

In 1977, a controversial Ir(III) complex of bipy²⁸ *i.e.* [Ir(bipy)₂(H₂O)(bipy)]Cl₃·3H₂O came in to picture. In this complex, the two bipyridine units were coordinated in bidentate fashion while the coordination of the third unit was a mystery. Just after the crystal structure of perchlorate salt of [Ir(bipy)₂(H₂O)(bipy)]₃ was reported²⁹ by Wickramasinghe, Bird and Serpone in 1981, suggested that one of the bipy ligand was rotated around the centre bond and coordinated in C[^]N fashion. Later, this fascinating and controversial structure [Ir(bipy)₂(bipy-H)]³⁺ was fully characterized by NMR and single crystal X-ray structure by Spellane, Watts and Curtis which was the first evidence of C[^]N coordination³⁰ of bipy through C-H activation.



The abnormal coordination κ^2 - N, C rather than normal κ^2 - N,N is known as rollover³¹ species. Till now, only a few metals, such as Pd(II)³², Au(III)³³, Rh(III)³⁴, Ir(III)³⁵, Pt(II)³⁶, and Cu(II)³⁷ are, to

be known for showing this behavior, out of them Ir(III) is still rare. The successful utilization of uncoordinated nitrogen in field of catalysis, C-C and C-H bond formation has been reported³⁸.

The emission color tuning of cyclometallated Ir(III) complexes can be done by introducing donor and acceptor groups in the ligand part³⁹. The pyridine being an electron rich species, which possibly be transformed into electron deficient with immediate protonation. The photo physical property of the Ir(III) complex with free pyridine ring could be tuned by simply protonation because of electron distribution will change.

In this report, we have focused on the syntheses and characterizations of an unusual rollover complex of iridium(III) and study of their emissive properties. The rollover complex is successfully employed for acid-base sensing applications. It also differentiates between acids with different pK_a values. We have successfully used the protonated complex as a probe for the detection of H-bonding. In addition, the excited state properties of these complexes were studied using DFT-based quantum chemical calculations.

EXPERIMENTAL SECTION

Materials: Iridium(III) chloride hydrate, 2,2'-bipyridine triphenylphosphine, 2-ethoxyethanol were purchased from Sigma Aldrich Chemical Company Ltd. Trifluoroacetic acid, acetic acid, hydrochloric acid, trifluoro methane sulphonic acid, triethylamine and all spectroscopic grade solvents DCM, methanol etc. were procured from Merck Company.

Characterization: ¹H NMR, ¹³C NMR and ³¹P NMR spectra were recorded in 400 MHz Bruker spectrometer using CDCl₃ as solvent and tetramethylsilane (TMS, $\delta = 0$ for ¹H and ¹³C NMR) and phosphoric acid (H₃PO₄, $\delta = 0$ for ³¹P NMR) as internal standard. Infra-red spectrum was recorded in FTIR Simadzu (IR prestige-21) and Perkin Elmer Spectrum 100 FTIR. UV-VIS absorption spectra were recorded in Simadzu Spectrophotometer (model UV-1800 and 2550). The steady state photoluminescence spectra were recorded on Spectrofluorometer FLS920-s Edinburgh. Elemental analyses were furnished on Elementar, VARIO III. Particle sizes of the nano-aggregates were determined on a Malvern Zetasizer (MAL1040152).

Cyclic voltammetry (CV) measurements were recorded on a CHI Potentiostat Model 604E. The platinum wire,

platinum and Ag/AgCl electrodes were used as counter, working and reference electrodes, respectively and the scan rate was maintained to 50mVs⁻¹. The complex was dissolved in acetonitrile (10 mL) and 0.1 M lithium perchlorate (LiClO₄) (100 Mg) was added to the solution (used as the supporting electrolyte). The whole experiment was conducted under inert atmosphere.

Syntheses of Complexes: To a stirred solution of IrCl₃·3H₂O (0.5025 mmol) in 2-ethoxyethanol (6 mL), triphenyl phosphine, (1.507 mmol) were added and the reaction mixture refluxed at 130°C for 4h. Then, 2,2'-bipyridine (1.252 mmol) was added along with Na₂CO₃ (1.507 mmol) to the reaction mixture which was further refluxed for 3h. The reaction mass was brought to room temperature. The resulting solid mass was contained two products, [Ir(bipy-H)(PPh₃)(H)(Cl)] and [Ir(N[^]N)(PPh₃)(H₂)Cl] which was purified by column chromatography and both products further recrystallized using a mixture of DCM and hexane (1:1) giving . The salt formation of rollover complex [Ir(bipy-H)(PPh₃)(H)(Cl)] was achieved simply by using TFA and BF₃·Et₂O simultaneously in DCM solvent.

[Ir(PPh₃)₂{(bipy-H)(Cl)(H)} or [Ir(bipy-H)] ¹H NMR (400 MHz, CDCl₃) δ 8.88 (d, *J* = 5.4 Hz, 1H), 7.89 (d, *J* = 7.8 Hz, 1H), 7.83 (d, *J* = 3.6 Hz, 1H), 7.52 – 7.36 (m, 13H), 7.17 (dt, *J* = 27.5, 7.2 Hz, 18H), 6.79 – 6.70 (m, 1H), 6.52 (d, *J* = 7.7 Hz, 1H), 5.85 (dd, *J* = 7.8, 4.5 Hz, 1H), -17.04 (t, *J* = 16.4 Hz, 1H); ¹³C NMR (101 MHz, CDCl₃) δ 163.21, 159.59, 149.37, 149.18, 140.41, 135.90, 133.99, 133.94, 133.88, 131.85, 131.59, 131.32, 129.12, 127.45, 127.40, 127.36, 124.38, 122.41, 119.77; ³¹P NMR (162 MHz, CDCl₃) δ 7.92, IR (KBr, cm⁻¹): 2100 (m, ν_{Ir-H}); ESI-HRMS calculated: C₄₆H₃₉ClIrN₂P₂ ([M+H]⁺): *m/z*, 909.1906, found: C₄₆H₃₉ClIrN₂P₂ ([M+H]⁺): *m/z*, 909.1938, Pale green solid; Yield, 60.00 % (Fig. S1).

[Ir(PPh₃)₂{(bipy-H)}(Cl)(H)].TFA or [Ir(bipy-H)H⁺].TFA ¹H NMR (400 MHz, CDCl₃) δ 9.01 (d, *J* = 4.9 Hz, 1H), 8.41 (d, *J* = 7.8 Hz, 1H), 8.07 (d, *J* = 4.2 Hz, 1H), 7.77 (t, *J* = 7.2 Hz, 1H), 7.52 – 7.37 (m, 10H), 7.33 – 7.11 (m, 17H), 7.10 – 6.98 (m, 1H), 6.70 (s, 1H), 6.16 (dd, *J* = 7.5, 5.3 Hz, 1H), δ -17.08 (t, *J* = 15.7 Hz, 1H); ¹³C NMR (101 MHz, CDCl₃) δ 157.70, 137.67, 133.69, 133.64, 133.58, 130.88, 130.61, 130.34, 129.91, 127.97, 127.92,

127.87, 125.48, 124.41, 121.71; ³¹P NMR (162 MHz, CDCl₃) δ 4.79, KBr, cm⁻¹): 2156 (m, ν_{Ir-H}); yellow solid; Yield, 96.00 % (Fig. S2).

[Ir(PPh₃)₂{(bipy-H)}(Cl)(H)].TFA or [Ir(bipy-H)H⁺].TFA ¹H NMR (400 MHz, DMSO) δ 8.88 (d, *J* = 5.1 Hz, 1H), 8.11 (d, *J* = 7.9 Hz, 1H), 8.00 (d, *J* = 4.8 Hz, 1H), 7.86 (t, *J* = 7.7 Hz, 1H), 7.49 – 7.11 (m, 33H), 6.98 (s, 1H), 6.55 (s, 1H), 6.18 (s, 1H), δ -17.18 (t, *J* = 15.9 Hz, 1H). ³¹P NMR (162 MHz, DMSO) δ 6.18 (Fig S3).

[Ir(PPh₃)₂{(bipy-H)}(Cl)(H)}H⁺BF₄⁻] or [Ir(bipy-H)H⁺BF₄⁻] ¹H NMR (400 MHz, CDCl₃) δ 9.00 (d, *J* = 5.3 Hz, 1H), 8.59 (d, *J* = 7.7 Hz, 1H), 8.24 (d, *J* = 5.3 Hz, 1H), 7.75 (t, *J* = 7.4 Hz, 1H), 7.41 (dt, *J* = 10.7, 5.3 Hz, 9H), 7.30 – 7.15 (m, 20H), 7.09 (d, *J* = 7.9 Hz, 1H), 7.01 (dd, *J* = 8.1, 4.9 Hz, 1H), 6.13 (dd, *J* = 7.8, 5.3 Hz, 1H), -17.06 (t, *J* = 15.8 Hz, 1H). ³¹P NMR (162 MHz, CDCl₃) δ 4.83 (Fig. S4).

[Ir(PPh₃)₂{(bipy-H)}(Cl)(H)}H⁺BF₄⁻] or [Ir(bipy-H)H⁺BF₄⁻] ¹H NMR (400 MHz, DMSO) δ 8.79 (d, *J* = 5.5 Hz, 1H), 7.97 (d, *J* = 7.5 Hz, 1H), 7.85 (d, *J* = 3.7 Hz, 1H), 7.72 (t, *J* = 8.2 Hz, 1H), 7.42 – 7.11 (m, 38H), 7.05 (t, *J* = 8.9 Hz, 1H), 6.67 (d, *J* = 4.3 Hz, 1H), 5.97 (d, *J* = 2.6 Hz, 1H), -17.19 (t, *J* = 16.1 Hz, 1H). ³¹P NMR (162 MHz, DMSO) δ 7.06 (Fig. S5).

Fabrication of thin-film on substrate for PL measurement

A 10⁻³M solution of each of the complexes (in THF) was prepared. 2-3 drops of the solution were placed on a thin glass substrate (2x2cm²). The solvent was allowed to evaporate slowly.

X-ray single crystal diffraction study

Single crystal X-ray diffraction data for the compounds **1** and **2** were recorded on Bruker AXS KAPPA APEX-II CCD and Rigaku Mercury375/M CD (XtaLAB mini) diffractometer respectively by using graphite Monochromated Mo – K_α radiation at 100.0(1) K by using Oxford cryosystem. The data sets collected Bruker AXS KAPPA APEX-II Kappa were collected using Bruker APEX-II suit,⁴⁰ data reduction and integration were performed by SAINT V7.685A12⁴⁰ (Bruker AXS, 2009) and absorption corrections and scaling was done

using SADABS V2008/112⁴⁰ (Bruker AXS). The data sets, which were collected on XtaLAB mini diffractometer, were processed with Rigaku Crystal Clear suite 2.0.⁴¹ The crystal structures were solved by using SHELXS2014⁴² and were refined using SHELXL2014⁴² available within Olex2.⁴³ All the hydrogen atoms have been geometrically fixed and refined using the riding model except the hydride anion, co-ordinating with Ir, which has been located from the difference Fourier map and were refined isotropically. All the diagrams have been generated using Mercury 3.1.1.⁴⁴ Geometric calculations have been done using PARST⁴⁵ and PLATON.⁴⁶

Computational Details

The DFT⁴⁷ and time-dependent DFT (TDDFT) studies were performed, for [Ir(bipy-H)] (For [Ir(bipy-H)].MeOH and Ir(bipy-H)·DCM (DCM = dichloromethane), only the ground state optimization have been done) and [Ir(bipy-H)H⁺], to know excited state electronic properties using Gaussian 09 program with B3LYP hybrid functional⁴⁸. A basis set of double-z quality (LANL2DZ) which is similar as the effective core potential of Hay and Wadt⁴⁹ has been used for Iridium. The TDDFT calculations were carried out with the same functional and basis sets to describe the electronic transitions to the low lying singlet and triplet states. All the calculations were performed in the presence of dichloromethane ($\epsilon=8.93$) with the Integral Equation Formalism - Polarizable Continuum Model (IEF-PCM) and the Gaussian 09 package.

Results and discussion

Herein, the iridium(III) complex has been synthesized by using 2, 2'-bipyridine as a chromophoric ligand. This idea was generated from our previous reports^{25a} where we have synthesized a series of cyclometalated complexes with tunable 'aggregation induced emission (AIE)' activity with employing a simple one-pot synthetic route. On pursuing intriguing features with varying chromophoric ligands retaining the same AIE framework, the one pot synthesis of iridium(III) chloride and triphenyl phosphine mixture with 2, 2'-bipyridine has resulted two emissive products. According to the thin layer chromatographic (TLC) study, it was observed that one of the products was nonpolar in nature with 0.5R_f using ethyl acetate-hexane mixture (2:3) while the other one giving 0.2R_f in methanol-DCM mixture (1:9). The ¹H NMR spectra of non polar complex (based on TLC study) are giving

eight different signals (**Fig. S1**) while the polar spot is giving five different signals (**Fig. S6**). The greater number of ¹H NMR signals in case of complex with nonpolar nature (on TLC plate) giving hints about its asymmetrical structure. While the ³¹P NMR spectra with one signal at $\delta = 7.92$ ppm is not giving any support in favour of structure of this unknown complex (**Fig. S1c**). The hydride ¹H NMR peaks were found triplet in nature because of P-H coupling ($J_{(P-H)} \sim 16.4$ Hz). The J-coupling value of J_{P-H} supports that hydride is *cis* to phosphorous in the complex. Anyway, these NMR studies is unable to enlighten the true structure of this unknown complex obtained with 2,2'-bipyridine. Further, the comparative structural study of the iridium(III) complex with 1,10 phenanthroline (N[^]N) is not giving any satisfactory clue to reveal the structure [where the complex with 1,10 phenanthroline has given two complexes with compositions, [Ir(PPh₃)₂(1,10-phen)(Cl)(H)] and [Ir(PPh₃)₂(1,10-phen)(H)(H)]^{25b}. After several worth full efforts, a single crystal of the unknown complex with trifluoroacetic acid (TFA) adduct was obtained. The single-crystal X-ray solution has revealed the first "AIP Rollover", where the displacement of one of the nitrogen atoms of bipyridine ligand followed by rotation of the pyridine ring is taking place, promoting the activation of the C-H bond (**Fig.1**) to give a five-membered cyclometalated complex, or "Rollover" complex [Ir(bipy-H)] (Scheme 1). The X-ray structure of the polar complex (based on the TLC plate study) confirms the normal mode of binding with 2, 2'-bipyridine *i.e.*, [Ir(N[^]N)(PPh₃)(H₂)Cl]. The detail synthetic techniques, photophysical property study and their bio-applications for this complex will be reported elsewhere. The plausible mechanism could be explained, the mixture of IrCl₃·xH₂O and triphenylphosphine will generate the four-membered cyclic complex with HCl as a side product. The addition of acid scavenger and 2, 2'-bipyridine in the reaction mixture will lead to the single protonation of pyridine ring in bipy and thus the protonated bipy ring will rotate and coordinate with iridium by κ^2 -N,C mode.

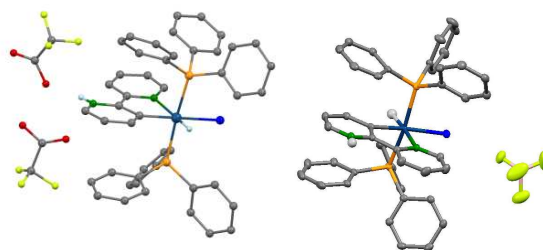
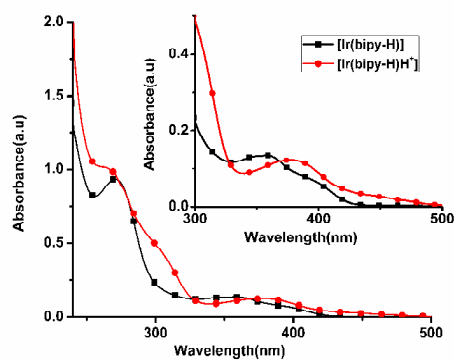
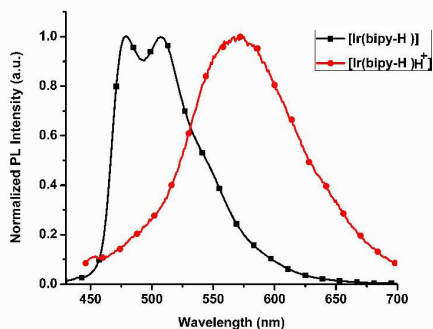


Fig. 1 ORTEP diagram for complexes, $[\text{Ir}(\text{bipy-H})\text{H}^+]\cdot\text{TFA}$ and $[\text{Ir}(\text{bipy-H})\text{H}^+\text{BF}_4^-]$ showing distorted octahedral geometry at the Ir site.

The emission and absorption spectra of $[\text{Ir}(\text{bipy-H})]$ were recorded with variation of different polarity of solvents, where there was not observed any change of emission/absorption with respect to polarity (**Fig. S7**). The UV-VIS absorption of $[\text{Ir}(\text{bipy-H})]$ and $[\text{Ir}(\text{bipy-H})\text{H}^+]$ in dichloromethane (DCM) shows higher energy bands at 270 (sh 290 nm) and 270 (sh 310 nm), respectively which can be identified as $\pi-\pi^*$ transitions.^{50a} The other set of bands were obtained for $[\text{Ir}(\text{bipy-H})]$ at 360 and 410 nm (**Fig. 2**) identified as metal-to-ligand charge transfer (¹MLCT and ³MLCT) transitions.^{50a} After addition of trifluoroacetic acid (TFA) into the complex solution of $[\text{Ir}(\text{bipy-H})]$, the broad MLCT transition band shifted from 360nm and 410nm to 380nm and 437nm, respectively⁵¹ (**Fig. 2**). During such process, the visible colour of the solution was changed from colourless to yellow after addition of TFA (**Fig. S8**).



a



b

Fig.2 (a)UV-VIS spectra of $[\text{Ir}(\text{bipy-H})]$ (1×10^{-5} M) in degassed DCM at room temperature before ($[\text{Ir}(\text{bipy-H})]$) and after the addition of TFA

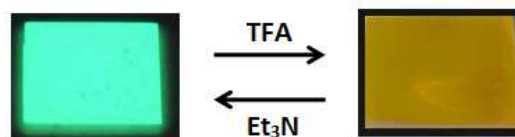
(inset: the same absorption spectrum is shown in shorter range); (b)

Emission spectra of $[\text{Ir}(\text{bipy-H})]$ and $[\text{Ir}(\text{bipy-H})\text{H}^+]$ in DCM solution.

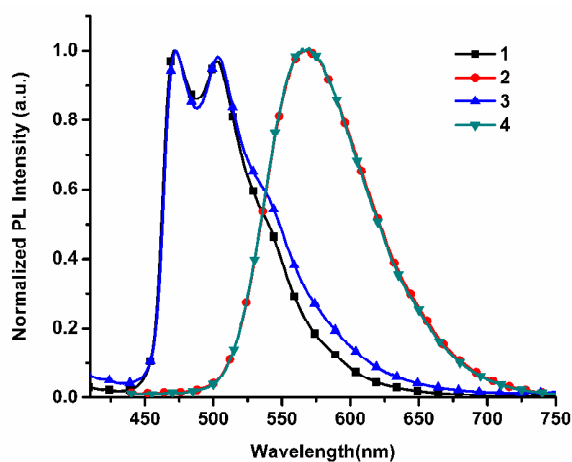
After protonation, the structured emission, where the low lying emissive states can be proposed of the closely spaced ³LC and ³MLCT emissive states,^{50b} changed into the featureless and broad emission spectra (**Fig. 2a**), a pure charge transfer (CT) states. After protonation, the contribution of ³LC state from lowest emitting states either has been completely lost or gets reduced. However, this facts are supported by DFT calculation which shows the LUMO orbitals of $[\text{Ir}(\text{bipy-H})\text{H}^+]$ is mainly localized on $(\text{bipy-H})^+$ (**Fig. S9**). The computational calculations (discussed later) along with the UV-VIS absorbance differences at lower energy (**Fig. 2a**) corroborate the facts that the formation of a new lower lying MLCT transition state in $[\text{Ir}(\text{bipy-H})\text{H}^+]$ which arise from the electronic transition from metal d orbitals to π^* lying on $(\text{bipy-H})^+$ along with a ligand-to-ligand charge transfer transition (LLCT) from the p-orbitals of chloro to π^* of $(\text{bipy-H})^+$ leading to a red shift in UV-VIS absorption spectra.

Reversible protonation and deprotonation

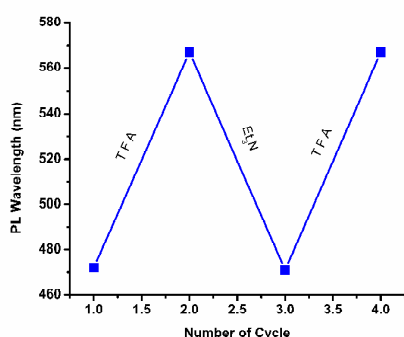
The yellowish-orange emitting complex ($\lambda_{\text{max}} = 569$ nm), $[\text{Ir}(\text{bipy-H})\text{H}^+]$ reverts to the bluish-green emitting $[\text{Ir}(\text{bipy-H})]$ ($\lambda_{\text{max}} = 475, 505$ nm) after addition of base (triethylamine) into the solution which substantiates the reversibility of this transition. The same experiment has been performed by using thin film of $[\text{Ir}(\text{bipy-H})]$. The thin film of $[\text{Ir}(\text{bipy-H})]$ after exposure to TFA vapour results λ_{max} at 569 nm a yellowish orange emission colour (**Fig. 3**). When a base Et_3N vapour was exposed to yellowish-orange emitting thin film of $[\text{Ir}(\text{bipy-H})\text{H}^+]\cdot\text{TFA}$, the bluish-green colour with λ_{max} at 475nm, 505nm was obtained. The repeated addition of acid or base to the complex, giving similar results which was proving, the reversible nature of protonation and deprotonation (**Fig. 3**).



a



i

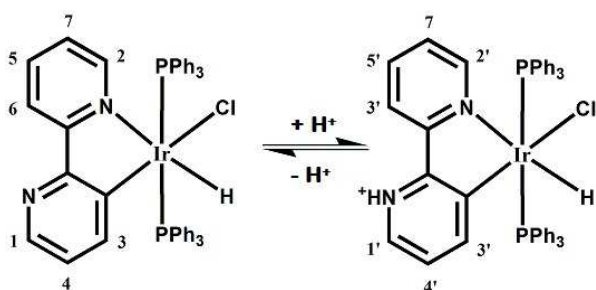


ii

b

5

Fig. 3 (a) Solid-state reversal of emission color of [Ir(bipy-H)] from blue-green to yellow-orange (on exposure to TFA) and the vice-versa (on exposure to Et₃N) (the photograph was taken under excitation of 365nm); b (i) Reversibility of solid-state emission spectrum of repeated
10 protonation and deprotonation by TFA and Et₃N exposure, respectively; (ii) Switching of emission wavelength (~569 nm to ~475 nm and vice versa) on exposure to TFA and Et₃N repeatedly, respectively



Scheme 1 Reversible protonation and deprotonation between [Ir(bipy-H)]
15 and [Ir(bipy-H)H⁺].

The protonation and deprotonation (**Scheme 1**) was also

confirmed by ¹H NMR spectra. The ¹H NMR spectra of [Ir(bipy-H)⁺] is recorded in CDCl₃, resulting more deshielded aromatic
20 protons of pyridyl [δ = 9.01 ppm (1), 8.41 ppm (2), 8.07 ppm (3), 7.77 ppm (4)] as compare to the protons of [Ir(bipy-H)], because the pyridyl ring of [Ir(bipy-H)H⁺] is positively charged (**Fig. 4**). After addition of Et₃N into [Ir(bipy-H)H⁺] and ¹H NMR of the resulting complex in CDCl₃ showed hardly any change of peak
25 positions in comparison with the original complex, [Ir(bipy-H)] (**Fig. 4**). The ¹H NMR spectra unequivocally supports the transformation of [Ir(bipy-H)] into [Ir(bipy-H)H⁺] which is completely reversible in nature .

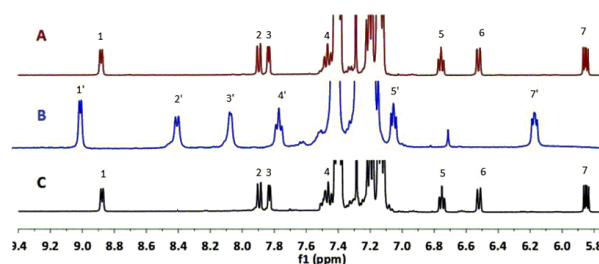


Fig. 4 ¹H NMR spectra of [Ir(bipy-H)] in CDCl₃ containing (A) 0 μ L trifluoroacetic acid (TFA) and (B) 100 μ L of TFA and (C) was obtained by adding 300 μ L of triethylamine (Et₃N) into (B).
30

Solvatochromic Probe

35 After protonation of [Ir(bipy-H)], the tendency to accept electrons / or -vely charged atoms of the pyridinium unit of [Ir(bipy-H)H⁺] has been multiplied. The pyridinium group shows affinity towards oxygen containing solvents. Taking advantage of this property, the complex, [Ir(bipy-H)H⁺] can be used as a
40 solvatochromic probes for detection of hydrogen-bond-accepting solvents (HBAS).

The UV-VIS absorbance (**Fig. S10**) and fluorescence spectroscopy studies have been performed to see the effect of HBAS on [Ir(bipy-H)H⁺]. As HBAS solvents, we have randomly chosen 1,
45 4-dioxane, diethyl ether, dimethylformamide (DMF), dimethylsulfoxide (DMSO), tetrahydrofuran (THF), methanol (CH₃OH) - which is capable of accepting H-bonds and DCM and chloroform (CHCl₃) are chosen as non-HBAS solvents. The emission spectra of [Ir(bipy-H)H⁺] is recorded using 1, 4-
50 dioxane, diethyl ether, DMF, DMSO, THF, CH₃OH, CHCl₃ and DCM as shown in **Fig. 5**. The emission spectrum in non HBAS solvents (DCM and CHCl₃) was observed as a featureless and broad emission with λ_{max} at 569 nm (**Fig.5**) which is similar to the

emission of $[\text{Ir}(\text{bipy-H})\text{H}^+]$, but the emission pattern was dramatically changed into the structured emission with λ_{max} at 475nm and 505nm with using HBAS solvents. In this case, the observed structured emission was found similar with the emission spectra of $[\text{Ir}(\text{bipy-H})]$. As the similar variation of emission spectra was observed in presence of non-polar solvents like, 1, 4-dioxane and diethyl ether along with the polar solvents (methanol, DMSO etc), the nature of interaction of the solvent molecules with pyridinium protons become independent of polarity of the solvents (**Fig. 5**).

The effective change in the emission spectra can be proposed to arise from the hydrogen bonding interactions between protonated form of pyridine ring, $[\text{Ir}(\text{bipy-H})\text{H}^+]$ with oxygen containing (H-bond acceptor) HBAS solvents. Due to hydrogen bonding interaction, the HBAS pulls hydrogen from the pyridinium ring of $[\text{Ir}(\text{bipy-H})\text{H}^+]$ which results a large emission shift exactly matching with the emission spectra of $[\text{Ir}(\text{bipy-H})]$.

The emission spectra of $[\text{Ir}(\text{bipy-H})\text{H}^+]$ was recorded in DCM (1×10^{-4} M) with gradual increasing amount of THF (0- 200 μ l) which clearly showing the fluorescence quenching with a hypsochromic emission shift (**Fig. 6**) and that is similar with the original emission of $[\text{Ir}(\text{bipy-H})\text{H}^+]$ [**Fig. 3b(i)**]. This experiment clearly supports the abstraction of proton from $[\text{Ir}(\text{bipy-H})\text{H}^+]$ which is transformed into $[\text{Ir}(\text{bipy-H})]$ with increasing concentration of THF.

Further, ^1H NMR study was performed to investigate the hydrogen bond interaction with oxygenated solvents. The ^1H NMR of $[\text{Ir}(\text{bipy-H})\text{H}^+]$ was recorded in CDCl_3 which showed the pyridinium NH^+ signal to, $\delta = 6.70$ ppm and the same signal was shielded to $\delta = 6.55$ ppm in DMSO-d_6 . The other proton signals 1' ($\delta = 9.01$ ppm), 2' ($\delta = 8.41$ ppm) and 3' ($\delta = 8.07$ ppm) in CDCl_3 were shielded and shifted to 1'' ($\delta = 8.88$ ppm), 2'' ($\delta = 8.11$ ppm) and 3'' ($\delta = 8.00$ ppm) in DMSO-d_6 (1', 2' and 3' protons are marked in **Scheme 1**; (**Fig. 7**)). In this case, DMSO having oxygen donor atom playing the role of a base which can interact with pyridinium NH^+ of $[\text{Ir}(\text{bipy-H})\text{H}^+]$ *i.e.*, Bronsted acid-base interaction.

In another case, ^1H NMR has been recorded for the complex of $[\text{Ir}(\text{bipy-H})\text{H}^+\text{BF}_4^-]$ in CDCl_3 and DMSO-d_6 , separately. ^1H NMR spectra was recorded in CDCl_3 of $[[\text{Ir}(\text{bipy-H})\text{H}^+\text{BF}_4^-]$ and found the chemical shift of NH proton of bipy appears at $\delta = 9.00$ ppm which in DMSO-d_6 changes to up-field ($\delta = 8.79$ ppm) (**Fig. S4a and S5a**). These results clearly indicating of the hydrogen bond

interaction playing between the NH^+ proton of $[\text{Ir}(\text{bipy-H})\text{H}^+]$ with HBAS which is Bronsted acid-base type interaction. On the other hand, the interaction playing between nitrogen lone pair of $[\text{Ir}(\text{bipy-H})]$ with BF_3 can be categorized as Lewis acid-base type of interaction.

Further, in support of this observation, we have optimized the geometry of $[\text{Ir}(\text{bipy-H})\text{H}^+]$ in presence of one molecule of methanol and in other case, with the presence of one molecule of dichloromethane (DCM) (**Fig S11**). The HOMO-LUMO energy gap of $[\text{Ir}(\text{bipy-H})\text{H}^+]\cdot\text{MeOH}$ (2.92 eV) was found to have higher energy value than the HOMO-LUMO energy gap of $[\text{Ir}(\text{bipy-H})\text{H}^+]\cdot\text{DCM}$ (2.84 eV) which is close to the HOMO-LUMO energy separation using the solvent DCM (HOMO-LUMO in DCM solvent = 2.76eV; **Table S2** and **Fig.S9**). This fact, further supports that the greater interaction is played between methanol with the proton of $[\text{Ir}(\text{bipy-H})\text{H}^+]$ as compared to interaction acting on dichloromethane.

The solid state thin film of $[\text{Ir}(\text{bipy-H})\text{H}^+]$ has been studied under exposure of volatile organic solvents (VOC's) like DMF, DMSO and other Hydrogen bond acceptor solvent (HBAS). The thin-film of $[\text{Ir}(\text{bipy-H})\text{H}^+]$ after exposing towards the solvents DMF, DMSO and other HBAS, the emission colour changes, yellowish-orange ($\lambda_{\text{max}} = 569\text{nm}$) to yellow ($\lambda_{\text{max}} = 555\text{nm}$) (**Fig. S12**). This transition is totally reversible under exposure the yellow emitting film to DCM at 70°C . The same reaction on carrying out in liquid phase, the original yellowish-orange colour of the solution turns into green (*vide infra*). In the present case, the different change of colour in solid-vapour phase reaction can be demonstrated by the incomplete deprotonation of $[\text{Ir}(\text{bipy-H})\text{H}^+]$. This property can be utilized for the detection of volatile organic compounds (VOCs).

The thin-layer chromatography (TLC) plate, a solid support has conveniently been used to see the effect of acid and base. The spot of the complex, $[\text{Ir}(\text{bipy-H})]$ on TLC plate shows bright bluish-green emission colour which was stable in presence of weakly acidic silica gel, but transformed into yellowish-orange colour in presence of TFA vapor. However, the yellowish-orange colour reverts to the original colour (bluish green) by abstraction of proton from $[\text{Ir}(\text{bipy-H})\text{H}^+]$ under exposure to triethylamine vapor (**Fig. S13**).

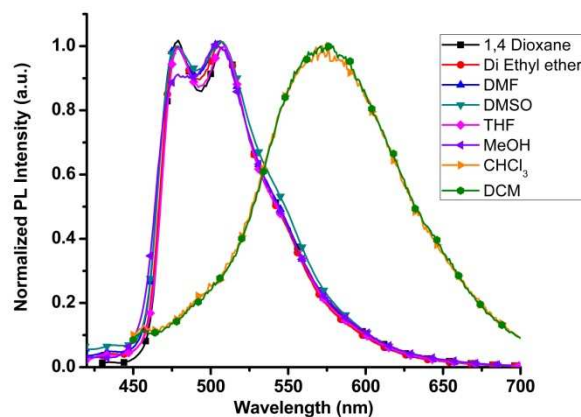


Fig. 5 Normalized emission spectra of $[\text{Ir}(\text{bipy-H})\text{H}^+]$ in different hydrogen bond donating solvents.

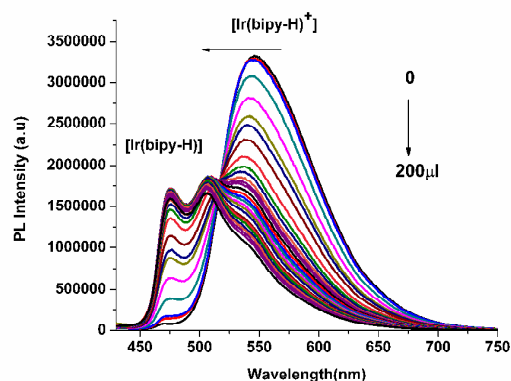


Fig.6 Emission of $[\text{Ir}(\text{bipy-H})^+]$ (1×10^{-4} in 2 mL CH_2Cl_2) with increasing amount of THF (0 -200 μl) was recorded, showing the transformation from $[\text{Ir}(\text{bipy-H})^+]$ to $[\text{Ir}(\text{bipy-H})]$.

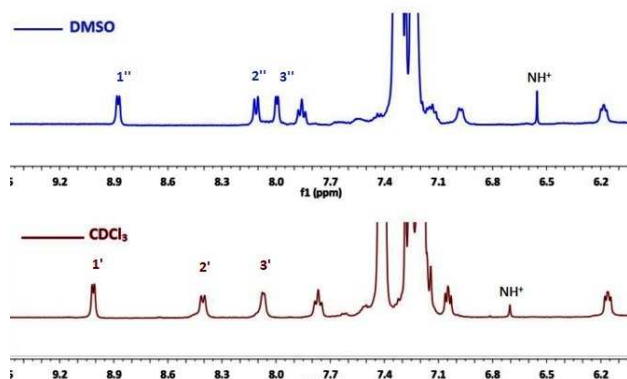


Fig.7 ^1H NMR spectra of $[\text{Ir}(\text{bipy-H})\text{H}^+]$ in CDCl_3 (top) and in DMSO (bottom) showing Hydrogen bond interaction between $[\text{Ir}(\text{bipy-H})\text{H}^+]$ and DMSO.

15

Ground state optimisation

The Geometry optimization for all complexes shows slightly distorted octahedral geometries where, the position of chloro ligand is *trans* to the carbon of bipyridine ring (**Fig. 8**). The crystal data of $[\text{Ir}(\text{bipy-H})\text{H}^+]$ are in good agreement with the optimized geometry of $[\text{Ir}(\text{bipy-H})\text{H}^+]$ in DCM. For comparison, the value computed for the bond length of Ir-P1 and Ir-C (2.40 and 2.02 \AA , respectively) is quite in agreement with the values obtained from X-ray values (2.34 and 1.99 \AA , respectively) (**Table S1**). Similarly, the computed bond angle between P1IrP2 and P1IrN (168.02 $^\circ$ and 94.92 $^\circ$, respectively) has been found to be in well matching with the X-ray values (174.20 $^\circ$ and 95.15 $^\circ$, respectively) (**Table S1**).

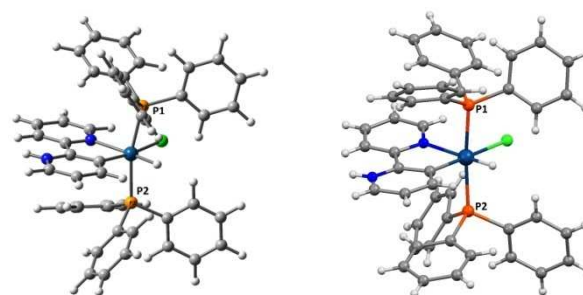


Fig. 8 The optimized Ground state molecular structure of $[\text{Ir}(\text{bipy-H})\text{H}^+]$ (Left) and single-crystal structure of $[\text{Ir}(\text{bipy-H})\text{H}^+]$ (right), optimization has been done at the B3LYP/cc-pVDZ level .

Excited States

The frontier molecular orbitals of $[\text{Ir}(\text{bipy-H})]$ are shown in (**Fig. 9**). The HOMO of this complex are located on Ir-d orbitals, chloro, the carbon bonded and little contribution on nitrogen bonded ring of bipyridine ligand (bipy-H). LUMO is mainly located on both pyridyl rings of bipyridine. These results support the existence of the metal-to-ligand charge-transfer (MLCT), ligand-centered (LC) transitions⁴⁶. The existence of HOMO on chlorine also supports the contribution of LLCT state to the lowest excited state. The HOMO orbitals of protonated complex $[\text{Ir}(\text{bipy-H})\text{H}^+]$ is quite different from $[\text{Ir}(\text{bipy-H})]$, is located on Ir-d orbitals, chloro and very small contribution on the carbon bonded ring of bipyridine ligand (bipy-H). While LUMO is

exclusively lying over pyridyl and pyridinium ring of [Ir(bipy-H)H⁺]. It shows the existence of a new lower-lying excited state in [Ir(bipy-H)H⁺] (Fig. S9), which is consisting of MLCT transition from the d orbitals of iridium(III) to the pyridinium ring of bipyridine ligand (bipy-H), interligand charge-transfer (LLCT) transition between the chloro ligand and bipyridine ligand (bipy-H)⁴⁷. The change in emission pattern, structured to broad and structureless upon protonation is caused by the significant reduction of contribution from the LC transition. The new low lying excited state results a visible and significant red shift in UV-VIS spectra (*vide infra*). The HOMO energies of both complexes having good agreement with oxidation potential measured using cyclic voltammetric study. The computed HOMO-LUMO gap for the complexes [Ir(bipy-H)] and [Ir(bipy-H)H⁺] is approximately 4.0 eV and 3.3 eV (Fig. S14, Table S2), respectively, which support the observed red shift in the emission spectra after protonation.

The TD-DFT calculation results were examined in detail, to gain more insight into the nature of the electronic transitions observed in the experimental absorption spectra. The calculated first excitation energies for [Ir(bipy-H)] and [Ir(bipy-H)H⁺] are found to be 3.42 eV (362 nm) and 2.76 eV (449 nm), respectively (Table S3). These values correlate satisfactorily to the observed red shift in absorption spectra (Fig. 2). This electronic transition can be seen as a promotion of an electron from the HOMO to the LUMO, with a significant MLCT character from the d orbitals of the Iridium to the π system of the bipyridine ligand together with ligand to ligand charge transfer from the p-orbital of the chlorine atom to the bipyridine ligand and a significant π to π^* transition within bipyridine ligand. The intense absorption band observed in the experimental spectra for [Ir(bipy-H)] at 300-370 nm corresponds mainly to the electronic transition (MLCT and LC) to the second excited singlet state (S₂) [360 nm (3.43 eV)]. The major contribution to this second singlet state is from HOMO to LUMO, with significant MLCT character. While a band 340-440 nm found for [Ir(bipy-H)H⁺] represents the similar types of transition with [420 nm (2.95 eV)].

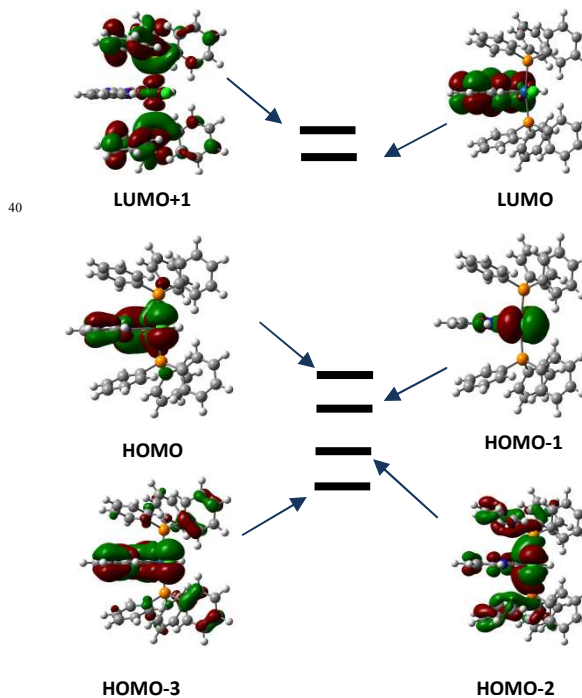


Fig.9 Highest and lowest occupied molecular orbitals of [Ir(bipy-H)]

The electrochemical behaviors of both complexes were measured by cyclic voltammetry (CV) in degassed acetonitrile containing 0.1 M LiClO₄ with a 0.05 V scan rate. Ferrocene/Ferrocenium ion⁺ (Fc/Fc⁺) has been used as an internal standard (F_c/F_c⁺ = 3.8V in acetonitrile). Both the complexes show irreversible oxidation as well as reduction waves (Fig S14). The anodic scan for both complexes was showing irreversible oxidation at 1.37V and 1.34V, respectively. The irreversibility in oxidation represents the redox couple of Ir(III)/Ir(IV) along with significant contribution of 'Ir-C' bonding in oxidation^{52a}. However, the cathodic scan shows irreversible reduction waves at -1.20V and -0.82V for [Ir(bipy-H)] and [Ir(bipy-H)H⁺] complexes, respectively (Fig.S11). The observed anodic shifts of [Ir(bipy-H)] and [Ir(bipy-H)H⁺] from -1.20V to -0.82V supports the increased electron withdrawing nature of pyridinium ion in [Ir(bipy-H)H⁺].

Aggregation Induced Phosphorescence

The AIP property of both complexes has been investigated. Complex **1** is showing very faint emission in dichloromethane (DCM), chloroform (CHCl₃), tetrahydrofuran (THF), dimethyl

sulfoxide (DMSO), 1,4 dioxane and dimethyl formamide (DMF) but showing very strong emission (λ_{max} at 475 and 505 nm) in solid state (under illumination with a 365 nm UV lamp) (**Fig. 3a**). The complex, [Ir(bipy-H)] is not soluble in water. The photoluminescent (PL) spectra of complex [Ir(bipy-H)] was studied in THF-water mixtures with different water fractions (f_w). The different amount of the water fraction, $f_w = 0-95\%$ are added to the solution of [Ir(bipy-H)] keeping the concentration same (1×10^{-4} M in THF). The PL intensity was gradually rising with increasing f_w . The maximum PL intensity was observed at $f_w=90\%$ which was showing approximately 14.5 times enhancement (**Fig.10**). As water was used as a non solvent, with increasing f_w in mixed solvent the complex may lead to formation of aggregated particle which was dispersed in THF. At higher f_w , the molecules come closer to form nano-aggregates and producing aggregation induced emission in the system. A control viscosity experiment has been performed using THF-Polyethylene glycol (PEG) mixture. The PL spectra of the complex have been recorded with increasing PEG fraction (f_{PEG}). The maximum PL intensity was observed in case of $f_{\text{PEG}} = 90\%$ which was 14.2 times higher than pure THF solution (**Fig S15**). The PEG is producing viscous medium which block the rotation of phenyl rotors in triphenylphosphine ligand in the solution, resulting the emission enhancement. The absolute quantum yield of [Ir(bipy-H)] in DCM solution and solid state were estimated and found to be 0.03% and 27.95%, respectively, which is about 931 times higher. Additionally, the photoluminescence lifetime of [Ir(bipy-H)] in THF and in 90% THF-Water was measured to be 3.33 and 12650 ns, respectively. Complex [Ir(bipy-H)] shows a very weak emission which is almost non luminescent in THF solvent. It happens due to rapid rotation of the triphenyl phosphine (rotor) which triggers a nonradiative transition in the system with a lowering of life-time as compared to its aggregated state. (**Fig.S16**). These facts prove its AIP character.

On the other hand, the emission behaviour of [Ir(bipy-H)] is totally different from [Ir(bipy-H)H⁺]. After exposure to trifluoroacetic acid (TFA), the maximum emission wavelength ($\lambda_{\text{max}} = 475, 505$ nm) of [Ir(bipy-H)] was red-shifted ($\lambda_{\text{max}} = 569$ nm for [Ir(bipy-H)H⁺]. The absorption band at 360 nm was shifted to 388 nm and a long tail was appeared in visible region. The oxygen containing solvents such as, MeOH, THF, DMSO etc. abstract protons from [Ir(bipy-H)H⁺] and it reverts to its original form. Whenever [Ir(bipy-H)H⁺] was dissolved in THF

or MeOH solvents to investigate AIP property (THF/Water, MeOH/Water or THF/ PEG, MeOH/Water), [Ir(bipy-H)H⁺] was converted into [Ir(bipy-H)] and finally at $f_w = 90\%$ or $f_{\text{PEG}} = 90\%$ results the same emission spectra as [Ir(bipy-H)]. This fact creates a problem to study AIP property of the protonated complex in THF-water.

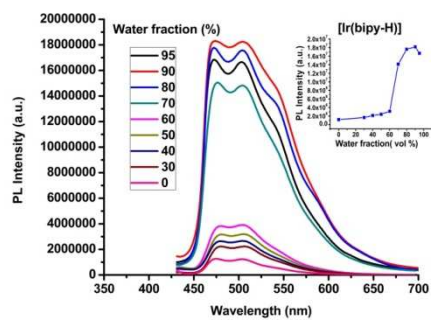
The protonation was achieved after acidifying THF. The emission colour of [Ir(bipy-H)] is changed to greenish-blue to bright yellow colour after using $f_w=90\%$ in acidic THF. [Ir(bipy-H)H⁺] produces green emission (under 365 nm UV lamp) at lower f_w which may be the mixture of both complexes. We have performed a controlled experiment where 5 equivalents of TFA was added to the AIE system of [Ir(bipy-H)] (TFA was added into 0-95% THF/water mixture of [Ir(bipy-H)]). The PL spectra have been recorded, showing the gradual emission enhancement with red shifting. The λ_{max} at 475nm and 505nm of [Ir(bipy-H)] is shifted to λ_{max} at 507nm and 532nm with gradual increasing water fraction, $f_w = 0-70\%$, respectively. The following water fractions, $f_w = 80, 90$ and 95% , shows the maximum emission wavelengths (λ_{max}) at 534nm, 538nm and 545 nm, respectively (**Fig. 11**). The PL intensity of $f_w = 90\%$ with TFA is 41 times higher than its $f_w = 0\%$ with TFA.

The viscosity experiment used to perform in THF-PEG mixture but in this case DCM-PEG mixture has been taken (as DCM is non oxygenated solvent). The PL intensity was recorded with increasing f_{PEG} . There is an enhancement in PL intensity with increasing f_{PEG} . The PL intensity of $f_{\text{PEG}} = 90\%$ having 17 times enhancement with respect to $f_{\text{PEG}} = 0\%$. The emission spectra without PEG is giving λ_{max} at 569 nm, but $f_{\text{PEG}} \geq 30\%$ is giving λ_{max} at 480 and 508 nm which supports the formation of [Ir(bipy-H)] (as PEG is capable of forming H-bond) (**Fig.S17**).

Two single crystals of [Ir(bipy-H)H⁺] \cdot TFA and Ir(bipy-H)H⁺BF₄⁻ were obtained from slow evaporation of DCM and Hexane mixture.

The structures of both the complexes have several short interactions (C-H \cdots O, C-H \cdots F and N⁺-H \cdots O in [Ir(bipy-H)H⁺] \cdot TFA and C-H \cdots π in [Ir(bipy-H)H⁺ BF₄⁻]. In the case of [Ir(bipy-H)H⁺] \cdot TFA, the shortest contact distances are within 2.34-2.90 Å, while the same for [Ir(bipy-H)H⁺ BF₄⁻] is 2.81 Å. The phenyl rings of triphenyl phosphine moiety were involved in all these short contacts (**Fig. 12**). Due to these intermolecular interactions involving the -PPh₃ group, the molecular motion of the phenyl rings of this group are restricted in the solid state.

Under such circumstances, the molecular motion of these groups will be restricted in solid state which will lead to close the non radiative path ways and subsequently open up several new radiative path ways. It has introduced the AIP property of both the complexes. Further studies using a particle size analyzer also put evidence the formation of nano aggregates, with diameters in the range of 0.17–2.0 nm (Fig. S18). Hence, this experiment clearly showing the increasing PL intensity arise due the aggregate formation, in other words, both complexes will be AIP-active.

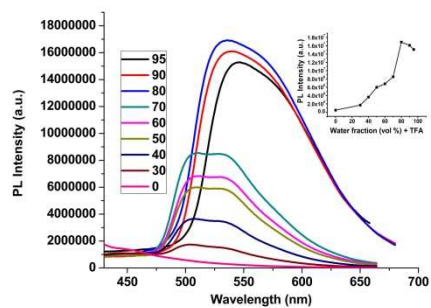


a



b

Fig.10 (a) Emission spectra of [Ir(bipy-H)] in THF/water mixtures [inset: intensity plot of intensity(*I*) values of [Ir(bipy-H)] versus the compositions of the aqueous mixtures], Concentration: 1×10^{-4} M; (b) Photographs of [Ir(bipy-H)] in THF/water mixtures with different water volume fractions (f_w) taken under UV illumination. excitation wavelength: 365 nm.

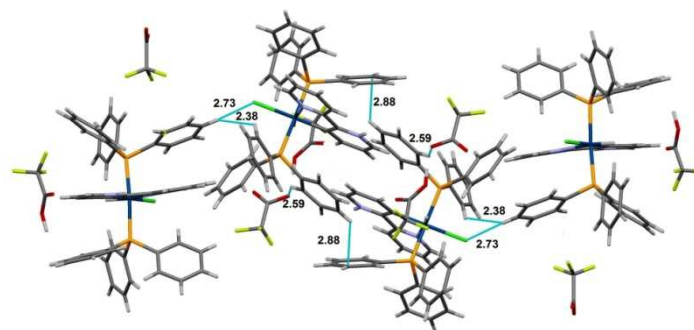


a

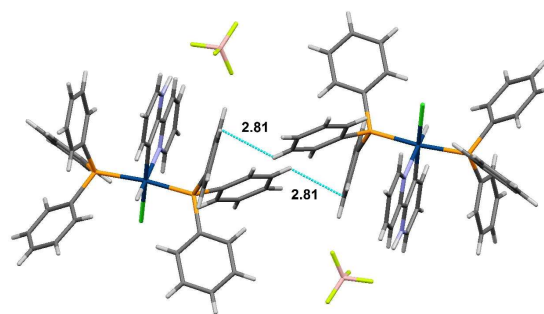


b

Fig.11 (a) Emission spectra of [Ir(bipy-H)] in (THF/water)+TFA mixtures [inset: plot of PL intensity (*I*) versus the compositions of the aqueous mixtures+ TFA] values of [Ir(bipy-H)] versus the compositions of the aqueous mixtures + TFA], Concentration: 1×10^{-4} M; (b) Photographs of [Ir(bipy-H)] in (THF/water)+TFA mixtures (f_w + TFA) taken under UV illumination (excitation wavelength: 365 nm).



a



b

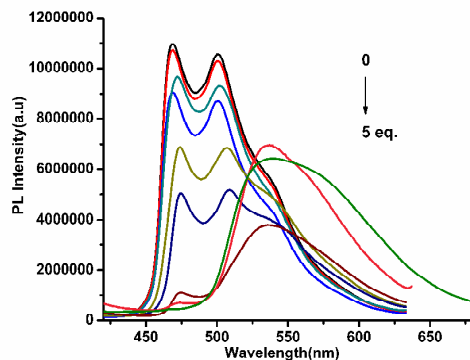
Fig. 12 Packing diagram for (a) [Ir(bipy-H)]⁺·TFA and (b) [Ir(bipy-H)]·BF₃, shows several interactions as shown in dashed lines. The unit cell of [Ir(bipy-H)]·TFA and [Ir(bipy-H)]⁺·BF₄⁻ contains four and two molecules, respectively.

Tunable AIP Property

The reversible protonation and deprotonation effect provide us an opportunity to observe the effect of pH on emission color. Unfortunately, the buffer solution with pH~1 is not able to result

full protonation of [Ir(bipy-H)] (**Fig. S19**). The tunable AIP property of [Ir(bipy-H)] has been observed with variation of acids. The color tuning of [Ir(bipy-H)] in the aggregate form has been observed simply by changing the pK_a of the acids. As we have already discussed about the AIP property in [Ir(bipy-H)]⁺ (*vide infra*), the TFA has been used in different water fraction of [Ir(bipy-H)] (in THF), showing AIP with maximum emission wavelength (λ_{max}) at 545 nm with $f_w = 95\%$ (**Fig.11**). In contrast, the solution of [Ir(bipy-H)]⁺ ($10^{-4}M$) in THF with $f_w = 95\%$ resulted the maximum emission wavelengths at 475nm and 505 nm (λ_{max}) while in the same solvent mixtures with addition of TFA (5 equivalent), the λ_{max} was changed to 545nm (**Fig.13 & S20**). The emission spectra of [Ir(bipy-H)] was recorded in DCM (instead of THF) and after complete acidification with TFA (used excess of TFA to saturate), the maximum emission wavelength was further red-shifted to 569 nm (**Fig. 2b**). The difference of emission spectra in THF and DCM in presence of TFA, indicates that the incomplete protonation of [Ir(bipy-H)] occurs in THF (which is capable of accepting protons) irrespective of the amount of a particular acid being used. This fact help us to understand that the extent of protonation to [Ir(bipy-H)] can be changed proportionately with the acids strength in mixture of solvents THF and water.

The addition of acids with different pK_a values in aggregated form of [Ir(bipy-H)] (in $f_w = 95\%$ in the mixture of THF and water) resulted a fine color tuning. After addition of acetic acid, the maximum emission wavelength remains unaltered, but with gradual increasing strength of acid [with pK_a , 0-(-12)] resulting a red shifted emission wavelength (**Fig. 13, 14**).



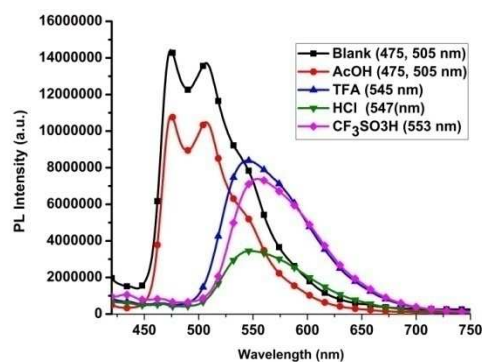
a



b

Fig. 13 (a) The PL spectra of [Ir(bipy-H)] after successive addition of acid (TFA) [0-5 equivalent] in the solution of [Ir(bipy-H)] in the mixture of THF and water with $f_w = 90\%$ concentration ($10^{-4}M$) and (b) the corresponding emission color under 365 UV lamp.

The emission spectra of [Ir(bipy-H)] are red shifted progressively with increasing acid concentration (TFA concentration). The structured peak at 470 and 505 nm was disappeared and the appearance of new broad peak at 545 nm, suggesting increasing extent of protonation occurs at higher concentration of acid (**Fig. 14**). The fine color tuning from 470 nm to 553 nm is totally dependent upon the population of both [Ir(bipy-H)] and [Ir(bipy-H)]⁺ species in the aggregate forms. In case of acetic acid, the population of [Ir(bipy-H)]⁺ is negligible which increased with increasing the pK_a of acids, so that the progressive increase of [Ir(bipy-H)]⁺ in the aggregate state is responsible for tuning of emission of the aggregated solution.



a



b

Fig. 14 (a) The PL spectra of [Ir(bipy-H)] with $f_w = 90\%$ concentration, (10^{-4} M) in the mixture of THF and water in presence of acids (5 eq.) with different pK_a , (Blank, Acetic acid, TFA, HCl and Triflic acid (left to right), respectively); (b) the emission color under 365 UV lamp.

Conclusions

We have reported the synthesis and characterization of first 'AIP ROLLOVER' complex of iridium(III). The reversible switching of emission can be obtained by simply protonation and deprotonation of [Ir(bipy-H)] and [Ir(bipy-H)H⁺], respectively. Further, the thin film of [Ir(bipy-H)] has, successfully been employed for detection volatile organic compounds (VOCs) with acidic and basic characters. The protonated form of [Ir(bipy-H)] has been convincingly proved to be used as H-bonding probes for the solvents capable of forming H-bond. Additionally, we have demonstrated the variation of emission wavelength of [Ir(bipy-H)] depending on the pK_a values acids. A single AIP material has been successfully employed as multi-responsive luminescent materials.

Acknowledgements

We thank the 'Department of Science and Technology (DST), Govt. of India' under a project (No: SR/S1/IC-48/2009), Council of Scientific and Industrial Research (CSIR) (No.01/2551/12/EMR-II), The 'UGC-SAP' and DST-FIST program for the chemistry department has been acknowledged for instrumental support. We, also thank IISER Mohali for the use of their single crystal X-ray diffraction and NMR research facilities and Special thanks to Dr. Ashish Gupta, Samtel Centre for Display Technologies, IIT Kanpur for solid state quantum yield measurement

AUTHOR INFORMATION

Corresponding Author

ir_laskar@bits-pilani.ac.in

^aDepartment of Chemistry, Birla Institute of Technology and Science, Pilani Campus, Pilani, Rajasthan, India, ir_laskar@bits-pilani.ac.in;

^bDepartment of Chemical Sciences, Indian Institute of Science Education and Research (IISER), Mohali, Sector 81, S. A. S. Nagar, Manauli PO, Mohali, Punjab 140306, India. angshurc@iisermohali.ac.in

50

Notes and references

Crystal data for [Ir(bipy-H)H⁺].TFA and [Ir(bipy-H)]H⁺.BF₄: the CIF file have been submitted to the Cambridge Crystallographic Data Centre (CCDC) CCDC numbers are 1030697 and 1030698 for [Ir(bipy-H)H⁺].TFA and [Ir(bipy-H)]H⁺.BF₄ respectively.

- (a) M. A. Baldo, M. E. Thompson and S. R. Forrest, *Nature*, 2000, **403**, 750; (b) C. Adachi, M. A. Baldo, M. E. Thompson and S. R. Forrest, *J. Appl. Phys.*, 2001, **90**, 5048; (c) P. T. Chou and Y. Chi, *Chem.-Eur. J.*, 2007, **13**, 380; (d) S. Lamansky, P. Djurovich, D. Murphy, F. Abdel-Razzaq, H. E. Lee, C. Adachi, P. E. Burrows, S. R. Forrest and M. E. Thompson, *J. Am. Chem. Soc.*, 2001, **123**, 4304.
- (a) Q. Zhao, C. H. Huang and F. Y. Li, *Chem. Soc. Rev.*, 2011, **40**, 2508; (b) M. X. Yu, Q. Zhao, L. X. Shi, F. Y. Li, Z. G. Zhou, H. Yang, T. Yi and C. H. Huang, *Chem. Commun.*, 2008, 2115; (c) L. Q. Xiong, Q. Zhao, H. L. Chen, Y. B. Wu, Z. S. Dong, Z. G. Zhou and F. Y. Li, *Inorg. Chem.*, 2010, **49**, 6402; (d) H. W. Liu, K. Y. Zhang, W. H. T. Law and K. K. W. Lo, *Organometallics*, 2010, **29**, 3474; (e) Y. Chen, L. Qiao, B. Yu, G. Li, C. Liu, L. Ji and H. Chao, *Chem. Commun.*, 2013, **49**, 11095; (f) P. Alam, G. Kaur, C. Climent, S. Pasha, D. Casanova, P. Alemany, A. R. Choudhury, I. R. Laskar, *Dalton Trans.*, 2014, **43**, 16431-16440; (g) Q. Zhao, F. Li and C. Huang, *Chem. Soc. Rev.*, 2010, **39**, 3007; (h) V. Guerschais and J.-L. Fillaut, *Coord. Chem. Rev.*, 2011, **255**, 2448; (i) G. G. Shan, D. X. Zhu, H. B. Li, P. Li, Z. M. Su and Y. Liao, *Dalton Trans.*, 2011, **40**, 2947; (j) X. Zhang, B. Li, Z.-H. Chen and Z.-N. Chen, *J. Mater. Chem.*, 2012, **22**, 11427; (k) O. S. Wenger, *Chem. Rev.* 2013, **113**, 3686; (l) A. Kobayashi and M. Kato, *Eur. J. Inorg. Chem.* 2014, 4469-4483.
- (a) C. H. Huang, F. Y. Li and W. Huang, *Introduction to Organic Light-Emitting Materials and Devices*, Press of Fudan University, Shanghai, 2005; (b) L. Flamigni, A. Barbieri, C. Sabatini, B. Ventura and F. Barigelletti, *Top. Curr. Chem.*, 2007, **281**, 143; (c) S. Lamansky, P. Djurovich, D. Murphy, F. Abdel-Razzaq, R. Kwong, I. Tsyba, M. Bortz, B. Mui, R. Bau and M. E. Thompson, *Inorg. Chem.*, 2001, **40**, 1704.
- Y. Kawamura, K. Goushi, J. Brooks, J. J. Brown, H. Sasabe and C. Adachi, *Appl. Phys. Lett.*, 2005, **86**, 071104.

90

- 5 R. B. Thompson, *Fluorescence Sensors and Biosensors*, CRC ,
Boca Raton 2006; S. M. Borisov, O. S. Wolfbeis, *Chem. Rev.* 50
2008, **108**, 423.
- 6 J. B. Birks, *Photophysics of Aromatic Molecules*, Wiley, London,
5 1970.
- 7 J. Mei, Y. Hong, J. W.Y. Lam, A. Qin, Y. Tang , and B. Z.Tang,
Adv. Mater. 2014, **26**, 5429.
- 8 W. Z.Yuan, Z-Q. Yu, Y. Tang, J. W. Y. Lam, N. Xie, P. Lu,
E.-Qi. Chen, and B. Z. Tang, *Macromolecules* 2011, **44**, 9618.
- 10 9 (a) M. C. Zhao, M. Wang, H. J. Liu, D. S. Liu, G. X. Zhang, D. Q.
Zhang and D. B. Zhu, *Langmuir*, 2009, **25**, 676; (b) W. X. Xue, G.
X. Zhang, D. Q. Zhang and D. B. Zhu, *Org. Lett.*, 2010, **12**, 2274;
60 (c) J. Liang, R. T. K. Kwok, H. Shi, B. Z. Tang and B. Liu, *ASC*
Appl. Mater. Interfaces, 2013, **5**, 8784; (d) H. B. Shi, R. T. K.
15 Kwok, J. Z. Liu, B. G. Xing, B. Z. Tang and B. Liu, *J. Am. Chem.*
Soc., 2012, **134**, 17972.
- 10 Y. Hong, J. W. Y. Lam and B. Z. Tang, *Chem. Soc. Rev.*, 2011, **40**,
5361; (b) D. Ding, K. Li, B. Liu and B. Z. Tang, *Acc. Chem. Res.*,
2013, **46**, 2441.
- 20 11 R. Dong, B. Zhu, Y. Zhou, D. Yan and X. Zhu, *Polym. Chem.*,
2013, **4**, 912.
- 12 W. Z. Yuan, Y.Gong, S. Chen, X. Y. Shen, J. W. Y. Lam, P. Lu,
Y. Lu, Z.Wang, R. Hu, N. Xie, H. S. Kwok, Y. Zhang, J. Z.Sun,
and B.Z. Tang, *Chem. Mater.*, 2012, **24**, 1518.
- 25 13 S. Li, Q. Wang , Y. Qian, S. Wang and Y. Li, G Yang, *J. Phys.*
Chem. A , 2007, **111**, 11793; (b) Q. Peng, Y. Yi, Z. Shuai, J. Shao,
J. Am. Chem. Soc., 2007, **129**, 9333; (c) Q. Peng, Y.Yi, Z. Shuai
and J. Shao, *J. Chem. Phys.*, 2007, **126**, 114302.
- 14 F. Würthner, T. E. Kaiser and C. R. Saha-Möller, *Angew.Chem.*,
30 *Int. Ed.*, 2011, **50**, 3376.
- 15 (a) R. Hu, E. Lager, A.A.-Aguilar, J. Liu, J. W. Y. Lam, H. H. Y.
Sung, I.D. Williams, Y.Zhong, K. S. Wong, E. P.-Cabrera, and B. Z.
Tang, *J. Phys. Chem. C*, 2009, **113**, 15845; (b) B.-R. Gao, H.-Y.
Wang, Y.-W. Hao, L.-M. Fu, H.-H. Fang, Y. Jiang, L. Wang, Q.-D.
35 Chen, H.Xia, L-Y.Pan, Y.-G. Ma, and H.-B. Sun, *J. Phys. Chem. B*
2010, **114**, 128.
- 16 (a) J. Wang, J. Mei, R. Hu, J. Z. Sun, A.Qin, and B. Z.Tang, *J.*
Am.Chem. Soc., 2012, **134**, 9956, (b) N.-W. Tseng, J. Liu, J. C. Y.
Ng, J. W. Y. Lam, Herman H. Y. Sung, Ian D.Williams, and B.
40 Z.Tang, *Chem. Sci.*, 2012, **3**, 493.
- 17 Y. Hong , J. W. Y. Lam and B. Z. Tang , *Chem. Commun.* 2009 ,
4332.
- 18 (a) Y.-Z. Xie, G.-G.Shan, P. Li, Z.-Y. Zhou, Z.-M. Su, *Dyes and*
Pigments, 2013, **96**, 467, (b) B. Xu, Z. Chi, X. Zhang, H. Li, C.
45 Chen, S. Liu, Y.Zhang and J.Xu, *Chem. Commun.*, 2011, **47**, 11080.
- 19 J.Liang, Z.Chen, L.Xu, J. Wang, J. Yin, G.-A Yu, Z.-N. Chen and
S.H.Liu, *J. Mater. Chem. C*, 2014, **2**, 2243.
- 20 (a) V. W.-W. Yam, K. M.-C. Wong and N. Zhu, *J. Am. Chem. Soc.*,
2002, **124**, 6506; (b) V. W.-W. Yam, K. H.-Y. Chan, K. M.- C. Wong
and N. Zhu, *Chem. Eur. J.*, 2005, **11**, 4535; (c) W. Lu, Y. Chen, V.
A. L. Roy, S. S.-Y. Chui and C.-M. Che, *Angew.Chem. Int. Ed.* 2009,
48, 7621; (d) H. Honda, Y. Ogawa, J. Kuwabara, and T. Kanbara, *Eur.*
J. Inorg. Chem., 2014, 1865; (e) S.Liu , H. Sun, Y. Ma, S. Ye , X. Z
Liu, X. Zhou, X. Mou, L.Wang, Q. Zhao and W.Huang, *J. Mater.*
55 *Chem.*, 2012, **22**, 22167.
- 21 J. Kuwabara, Y. Ogawa, A. Taketoshi, T. Kanbara, *J. Organomet.*
Chem., 2011, 696, 1289.
- 22 C. Zhu, S.Li, M. Luo, X. Zhou, Y.Niu, M. Li, J. Zhu, Z. Cao ,
X.Lu,
60 T. Wen, Z. Xie, P. V. R. Schleyer and H. Xia, *Nat. Chem.*, 2013, 5,
698.
- 23 X.-L. Xin, M. Chen, Y.-b. Ai, F.-L. Yang, X.-L.Li, and F. Li, *Inorg.*
Chem., 2014, **53**, 2922.
- 24 (a) G.-G. Shan, D.-X. Zhu, H.-B. Li, P. Li, Z.-M. Su and Y. Liao,
65 *Dalton Trans.*, 2011, **40**, 2947; (b) Y. You, H. S. Huh, K. S. Kim, S.
W. Lee,D. Kim and S. Y. Park, *Chem. Commun.*, 2008, 3998; (c) Q.
Zhao, L. Li, F. Li, M. Yu, Z. Liu, T. Yi and C. Huang, *Chem.*
Commun., 2008, 685.
- 25 (a) P. Alam, P. Das, C. Climentc, M. Karanam, D.Casanovac, A. R.
Choudhury, P. Alemany, N. R. Jana and I. R. Laskar, *J. Mater. Chem*
70 *C*, 2014, **2**, 5618; (b) P. Alam, M. Karanam, D. Bandyopadhyay, A. R.
Choudhury and I. R. Laskar, *Eur. J. Inorg. Chem.* 2014, **23**, 3710; (c)
P. Alam, M. Karanam, A. Roy Choudhury and I. R. Laskar, *Dalton*
Trans., 2012, 9276; (d) X.-G.Hou, Y. Wu, H.-T. Cao, H.-Z. Sun, H.-B.
75 Li, G.-G. Shan and Z.-M. Su, *Chem. Commun.*, 2014, **50**, 6031;(e) N.
Zhao, Y.-H. Wu, J. Luo, L.-X. Shia and Z.-N.Chen, *Analyst*, 2013, **138**,
894.
- 26 C. M. Flynn and J. N. Demas, *J. Am. Chem. Soc.*, 1974, **96**, 1959–
1960.
- 80 27 (a) M. A. Cinellu, A.Zucca, S.Stoccoro, G.Minghetti, M.Manassero
and M.Sansoni, *J. Chem. Soc. Dalton Trans.*, 1996, 4217; (b)
R.Uson, J.Fornies, M.Tomas, J. M.Casas and C.Fortuño, *Polyhedron*,
1989, **8**, 2209.
- 28 R. J. Watts, J. S. Harrington and J. Van Houten, *J. Am. Chem. Soc.*,
85 1977, **99**, 2179.
- 29 W. A. Wickramasinghe, P. H. Bird and N. Serpone, *J. Chem. Soc.*,
Chem. Commun., 1981, 1284.
- 30 P. J. Spellane, R. J. Watts and C. J. Curtis, *Inorg. Chem.*, 1983, **22**,
4060–4062.
- 90 31 B. Butschke and H.Schwarz, *Chem. Sci.*, 2012, **3**, 308.
- 32 (a) G. Minghetti, A.Doppiu, A.Zucca, S.Stoccoro, M. A.Cinellu,
M.Manassero and M. Sansoni, *Chem. Heterocycl. Compd.* 1999, **35** ,
992; (b) G. L.Petretto, A.Zucca, S.Stoccoro, M. A.Cinellu and
G. J. Minghetti, *Organomet. Chem.* 2010, **695**, 256; (c) G. L. Petretto,
95 J. P. Rourke, L. Maidich, S.Stoccoro, M. A.Cinellu,G.Minghetti, G.
J. Clarkson, and A. Zucca, *Organometallics*, 2012, **31**, 2971.

- 33 F.Cocco, M. A.Cinellu, G.Minghetti, A.Zucca, S.Stoccoro, L.Maiore and M.Manassero, *Organometallics*, 2010, **29**, 1064.
- 34 M. L. Zuber and F. P. Pruchnik, *Polyhedron*, 2006, **25**, 2773.
- 35 (a) K. J. H. Young, O. A. Mironov and R. A. Periana, *Organometallics*, 2007, **26**, 2137; (b) K. J. H. Young, M. Yousuffuddin, D. H. Hess, R. A. Periana, *Organometallics*, 2009, **28**, 3395.
- 36 (a) A. C. Skapski, V. F. Sutcliffe and G. B. Young, *J. Chem. Soc. Chem. Commun.*, 1985, 609; (b) G. Minghetti, S. Stoccoro, M. A. Cinellu, B. Soro and A. Zucca, *Organometallics*, 2003, **22**, 4770; (c) A. Doppiu, G. Minghetti, M. A. Cinellu, S. Stoccoro, A. Zucca, and M. Manassero, *Organometallics*, 2001, **20**, 1148; (d) G. J. P. Britovsek, R. A. Taylor, G. J. Sunley, D. J. Law, and A. J. P. White, *Organometallics*, 2006, **25**, 2074; (e) S. H. Crosby, G. J. Clarkson, and J. P. Rourke, *Organometallics*, 2011, **30**, 3603; (f) L. Maidich, G. Zuri, S. Stoccoro, M. A. Cinellu and A. Z. Dal, *Dalton Trans.*, 2014, DOI: DOI: 10.1039/c4dt02080d.
- 37 J.-W. Zhao, C.-M. Wang, J. Zhang, S.-T. Zheng and G.-Y. Yang, *Chem.–Eur. J.*, 2008, **14**, 9223.
- 38 (a) B. Butschke, S. G. Tabrizi and H. Schwarz, *Int. J. Mass Spectrom.*, 2010, **291**, 125–132. (b) B. Butschke, S. G. Tabrizi and H. Schwarz, *Chemistry*, 2010, **16**, 3962; (c) B. Butschke and H. Schwarz, *Organometallics*, 2010, **29**, 6002; (d) B. Butschke, and H. Schwarz, *Int. J. Mass Spectrom.*, 2011, **306**, 108.
- 39 Y. Chi and P.-T. Chou, *Chem. Soc. Rev.*, 2010, **39**, 638.
- 40 APEX2; SADABS; SAINT; Bruker AXS Inc.: Madison, Wisconsin, USA, 2008.
- 41 CrystalClear 2.0, Rigaku Corporation, Tokyo, Japan
- 42 G. M. Sheldrick, *Acta Crystallogr.* 2015, **C71**, 3.
- 43 O. V. Dolomanov, L. J. Bourhis, R. J. Gildea, J. A. K. Howard and H. Puschmann, *J. Appl. Cryst.* 2009, **42**, 339.
- 44 A. L. Spek, *Acta Crystallogr.* 2009, **D65**, 148.
- 45 M. Nardelli, *J. Appl. Cryst.* 1995, **28**, 569.
- 46 A. L. Spek, *Acta Crystallogr.* 2009, **D65**, 148.
- 47 A. D. Becke, *J. Chem. Phys.* 1993, **98**, 5648.
- 48 M. J. Frisch, G. W. Trucks, H. B. Schlegel, G. E. Scuseria, M. A. Robb, J. R. Cheeseman, G. Scalmani, V. Barone, B. Mennucci, G. A. Petersson, H. Nakatsuji, M. Caricato, X. Li, H. P. Hratchian, A. F. Izmaylov, J. Bloino, G. Zheng, J. L. Sonnenberg, M. Hada, M. Ehara, K. Toyota, R. Fukuda, J. Hasegawa, M. Ishida, T. Nakajima, Y. Honda, O. Kitao, H. Nakai, T. Vreven, J. A. Montgomery, Jr, J. E. Peralta, F. Ogliaro, M. Bearpark, J. J. Heyd, E. Brothers, K. N. Kudin, V. N. Staroverov, R. Kobayashi, J. Normand, K. Raghavachari, A. Rendell, J. C. Burant, S. S. Iyengar, J. Tomasi, M. Cossi, N. Rega, N. J. Millam, M. Klene, J. E. Knox, J. B. Cross, V. Bakken, C. Adamo, J. Jaramillo, R. Gomperts, R. E. Stratmann, O. Yazyev, A. J. Austin, R. Cammi, C. Pomelli, J. W. Ochterski, R. L. Martin, K. Morokuma, V. G. Zakrzewski, G. A. Voth, P. Salvador, J. J. Dannenberg, S. Dapprich, A. D. Daniels, Ö. Farkas, J. B. Foresman, J. V. Ortiz, J. Cioslowski and D. J. Fox, *Gaussian 09, Revision D.01*, Gaussian, Inc., Wallingford, CT, 2009
- 49 (a) P. J. Hay and W. R. Wadt, *J. Chem. Phys.*, 1985, **82**, 270-283; (b) W. R. Wadt and P. J. Hay, *J. Chem. Phys.*, 1985, **82**, 284-298; (c) P. J. Hay, and W. R. Wadt, *J. Chem. Phys.*, 1985, **82**, 299-311.
- 50 (a) P. Alam, I. R. Laskar, C. Climent, D. Casanova, P. Alemany, M. Karanam, A. R. Choudhury and J. R. Butcherd, *Polyhedron*, 2013, **53**, 286; (b) M. V. Werrett, S. Muzzioli, P. J. Wright, A. Palazzi, P. Raiteri, S. Zacchini, M. Massi, and S. Stagni, *Inorg. Chem.*, 2014, **53**, 229.
- 51 A. Nakagawa, Y. Hisamatsu, S. Moromizato, M. Kohno and S. Aoki, *Inorg. Chem.*, 2014, **53**, 409.
- 52 D. L. Davies, F. Lelj, M. P. Lowe, K. S. Ryder, K. Singh and S. Singh, *Dalton Trans.*, 2014, **43**, 4026; (b) K. Hasan, L. Donato, Y. Shen, J. D. Slinker and E. Z.-Colman, *Dalton Trans.*, 2014, **43**, 13672.